Data-Driven Gas Sensing Performance of Sn-Doped NiO Thin Films

Tahseen H. Mubarak[1], Hiba Rashid Shakir[2], Fikrat Hikmat Jasim[3], Shaymaa A. Hussein[4], Nadir Fadhil Habubi[3, 5, 6], Sami Salman Chiad[3] and Yassin Hasan Kadhim[7]

[1]*Department of Physics, College of Science, University of Diyala, 32001 Baqubah, Iraq*
[2]*Department of Optometry, Technical Medical Institute - Al-Mansur, Middle Technical University, 10001 Baghdad, Iraq*
[3]*Department of Physics, College of Education, Mustansiriyah University, 10052 Baghdad, Iraq*
[4]*Department of Medical Laboratory Techniques, Al-Manara College for Medical Sciences, 62001 Amarah, Iraq*
[5]*Department of Radiation and Sonar Technologies, Alnukhba University College, 10001 Baghdad, Iraq*
[6]*Department of Radiology Techniques, Al-Qalam University College, 36001 Kirkuk, Iraq*
[7]*Department of Optics Techniques, College of Health and Medical Techniques, Al-Mustaqbal University, 51001 Hillah, Iraq*
prof.dr.tahseen@uodiyala.edu.iq, hiba.rashid@mtu.edu.iq, fikrat@uomustansiriyah.edu.iq, nadirfadhil@uomustansiriyah.edu.iq, shams@uotechnology.edu.iq, dr.sami@uomustansiriyah.edu.iq, yassin.hasan@uomus.edu.iq

Keywords: Nio, Sn Doping, CSP, Gas Sensing, Structural Properties, Optical Properties.

Abstract: This study explores the influence of tin (Sn) doping at concentrations of 0%, 2%, and 4% synthesized via chemical spray pyrolysis (CSP) at 400°C. XRD analysis verified the construction of a cubic NiO phase with strong peaks that match the (111), (200), and (220) planes. Sn incorporation enhanced crystallinity, as evidenced by a raise in grain size from 13.14 nm (undoped) to 17.51 nm (4% Sn), along with a decrease in dislocation density (from 58.53 to 45.71 × 10^{14} lines/m²) and lattice strain (from 29.63 to 25.37 × 10^{-4}). Atomic force microscopy (AFM) analysis revealed a smoother film surface with increasing Sn content, indicated by a reduction in average surface roughness from 11.71 nm to 4.83 nm. Optical characterization showed a decrease in both the optical bandgap (from 3.86 eV to 3.75 eV) and transmittance (from 96.1% to 89.5%) as Sn concentration increased, attributed to defect-related absorption. Gas-sensing measurements revealed that undoped NiO exhibited the highest hydrogen sensitivity (29.56% at 225 ppm), which diminished to 12.3% for films doped with 4% Sn, likely due to enhanced charge carrier recombination. These findings emphasize the balance between improved structural and optical properties and reduced gas sensitivity, identifying undoped NiO as the most effective candidate for hydrogen sensing applications.

1 INTRODUCTION

NiO films have gained significant research interest owing to their wide-ranging industrial uses [1], [2]. As a wide bandgap of (3.6-4.0 eV), NiO demonstrates excellent suitability for electronic and optical applications. Particularly noteworthy is its p-type semiconducting nature, which makes it highly desirable for optical window applications requiring efficient hole injection [3]-[5]. Nickel oxide films have a wide range of uses, including, electrochromic display devices [6], [7], anode material [8], and functional layer sensors [9]-[12]. Thin films of nickel oxide can be fabricated through various deposition techniques, each offering distinct advantages for different applications. Common preparation methods include pulsed laser deposition (PLD) [13], laser beam evaporation [14], and magnetron sputtering [15]-[17]. Additional approaches encompass laser ablation [18], thermal evaporation [19], [20], sol-gel processing [21], chemical vapor deposition (CVD) [22], [23], and chemical spray pyrolysis (CSP), [13], [24]. This diversity of fabrication methods enables precise control over film properties to meet specific application requirements. Among various fabrication techniques, spray pyrolysis has emerged as a particularly effective method for producing high-quality NiO thin films. This simple and cost-effective approach enables large-area deposition with excellent uniformity while maintaining good electronic properties. CSP technique has demonstrated remarkable success in preparing various metal oxide thin films [25], making it an ideal choice for this investigation. In the present study, we employed CSP

to fabricate undoped NiO films as a baseline for examining how tin (Sn) doping influences the structural characteristics, morphological features, and optical properties of the deposited films.

2 EXPERIMENTAL

Tin-doped nickel oxide films were fabricated using CSP technique with precise control of deposition parameters. The precursor solution was obtained by dissolving 0.1 M nickel acetate ($Ni(CH_3COO)_2$) in 100 ml deionized water, with tin nitrate ($Sn(NO_3)_2$) added to achieve doping concentrations of 2% and 4%. Films were grown on substrates maintained at 400°C under optimal circumstances: 6-second spraying intervals followed by 1.5-minute cooling periods, a deposition rate of 9 ml/min, a nozzle-to-substrate distance of 28±1 cm, and air carrier gas at 5 bar pressure. The resulting films exhibited uniform thicknesses of 300±20 nm as measured by Stellar Net TF method. Comprehensive characterization was performed using multiple analytical techniques. Crystal structure analysis was conducted via XRD (Shimadzu XRD-6000). Surface morphology was examined using AFM (SPM-AA3000, Angstrom Advanced Inc.). Optical properties were measured across 300-900 nm wavelengths using a Shimadzu UV-Vis spectrophotometer. Gas sensing performance was evaluated by monitoring resistance changes in a custom cylindrical test chamber (8.5 cm radius × 17 cm height) under controlled hydrogen exposure.

3 RESULTS AND DISCUSSIONS

Figure 1 presents the X-ray diffraction patterns comparing undoped NiO with Sn-doped (NiO:Sn) films, clearly demonstrating structural modifications induced by tin incorporation. Three main diffraction peaks are observed at 2θ values of 37.92°, 43.83°, and 62.74°, corresponding to the (111), (200), and (220) crystallographic planes. These peaks are in excellent agreement with ICDD card No. 04-0835 [26], confirming the formation of phase-pure NiO with a face-centered cubic (FCC) structure.

The introduction of Sn dopants significantly modifies the crystalline properties of the films in two main ways. First, the increase in peak intensity with rising Sn concentration (from 2% to 4%) indicates improved crystallinity. This enhancement may be attributed either to dopant-assisted grain growth through improved atomic rearrangement during deposition, or to the occupation of interstitial sites by Sn ions, which enhances long-range ordering in the crystal lattice [27], [28]. Second, the observed shift in peak positions, particularly for the dominant (200) reflection, suggests a modification of lattice parameters caused by substitution of Ni^{2+} ions with slightly larger Sn^{4+} ions. This substitution introduces controlled lattice strain while preserving the overall cubic symmetry.

The crystallographic properties of the films were quantitatively analyzed using standard XRD approaches. The crystallite size was found to increase progressively from 13.14 nm to 17.51 nm with increasing Sn content [29], [30], [31]. This trend indicates that Sn doping promotes crystal growth, likely by reducing nucleation density and enhancing atomic mobility during film formation.

The dislocation density was also evaluated using a standard relation [32]. The values decreased from 58.53×10^{14} to 45.09×10^{14} m^{-2} as Sn concentration increased [32], [33]. This reduction in defect density suggests that tin incorporation improves crystalline quality by reducing lattice imperfections and grain boundary discontinuities.

The lattice strain, evaluated using a standard XRD-based relation [33], shows a gradual decrease with increasing tin content. The strain values decrease from 29.63×10^{-4} to 25.37×10^{-4} [34], [35]. This reduction indicates strain relaxation within the crystal lattice, suggesting that Sn dopants help relieve internal stress in NiO films. This effect may arise from either substitutional incorporation of Sn ions or their accommodation at interstitial sites, leading to partial compensation of lattice distortions.

Table 1: D, E_g, and S_{par} of prepared films.

Specimen	2 q (°)	(hkl) Plane	FWHM (°)	E_g (eV)	*D* (nm)	δ (× 10^{14}) (lines/m^2)	ε (× 10^{-4})
NiO	37.92	111	0.78	3.86	13.14	58.53	29.63
NiO: 2% Sn	37.88	111	0.73	3.82	15.81	51.09	27.02
NiO: 4% Sn	37.83	111	0.67	3.75	17.51	45.71	25.37

The overall structural parameters, summarized in Table 1 and Figure 2, collectively demonstrate that tin doping improves the crystalline quality of NiO films. The reduction in FWHM, the increase in crystallite size, and the simultaneous decrease in dislocation density and lattice strain all indicate enhanced long-range atomic ordering. These improvements are attributed to the ability of Sn dopants to influence nucleation behavior and grain growth dynamics during spray pyrolysis deposition.

The surface morphology of both undoped and Sn-doped NiO films was further investigated using atomic force microscopy (AFM), providing three-dimensional topographical information that complements the XRD results. As shown in Figure 3, all films exhibit uniform, dense, and crack-free surfaces with homogeneous particle distribution, confirming high-quality film growth via spray pyrolysis. AFM analysis reveals significant changes in surface properties with tin incorporation. The average particle size decreases markedly from 87.4 nm for undoped NiO to 46.5 nm for films doped with 4% Sn, corresponding to a reduction of about 46.8%. In addition, surface roughness parameters also improve, with root mean square roughness decreasing from 5.86 nm to 3.16 nm for the highest Sn concentration.

The particle sizes obtained from AFM are consistently larger than those calculated from XRD (Table 2). This difference is expected because AFM measures actual surface features, which may consist of several crystallites, whereas XRD determines coherent diffraction domains. Such discrepancies are widely reported in the literature [36], [37] and confirm the polycrystalline nature of the films, where each surface particle observed in AFM can be composed of multiple smaller crystallites detected by XRD [38].

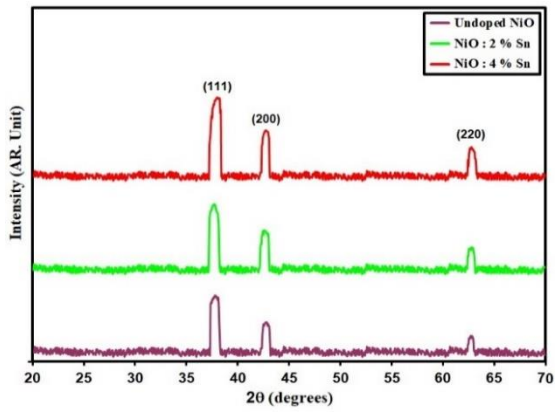

Figure 1: XRD styles of deposit films.

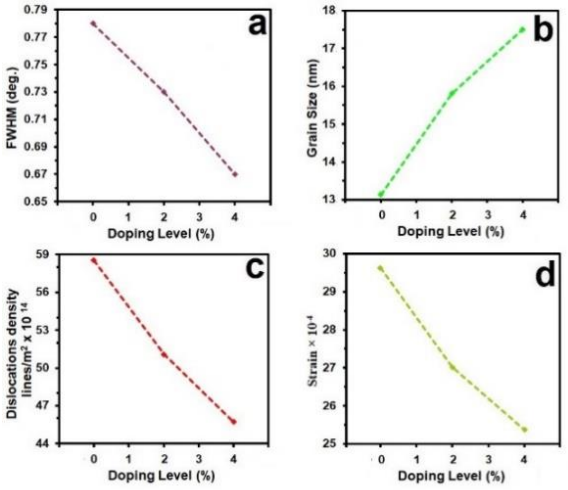

Figure 2: FWHM (a) D (b) δ (c) ε (d) of the grown films.

Table 2: AFM parameters of deposit films.

Specimen	P_{av} nm	R_a (nm)	R. M. S. (nm)
NiO	87.4	11.71	7.76
NiO: 2% Sn	84.6	5.58	5.90
NiO: 4% Sn	46.5	4.83	2.39

The optical characterization of the films reveals significant doping-dependent behavior, as illustrated in Figure 4. NiO films exhibit high visible-light transparency of 96.1%, which gradually decreases to 92.8% and 89.5% with 2% and 4% Sn doping, respectively [39]–[41]. The high transmittance in the visible region confirms good optical quality of the films, making them suitable for transparent electronic and optoelectronic applications. This reduction in optical transmission is associated with increased light absorption, as described by the standard relationship between absorbance and transmittance [43].

Figure 5 illustrates the dependence of absorbance on wavelength. The films show higher absorbance in the ultraviolet region and lower values in the visible range [42], [43]. In addition, increasing tin concentration leads to higher absorbance values. This behavior is attributed to increased optical density and the formation of localized states within the band structure, which enhance photon absorption, particularly in the UV region.

The absorption coefficient, an important parameter describing light–matter interaction, was determined using a standard relation involving absorbance and film thickness [43]. Figure 4 shows that the absorption coefficient decreases with increasing Sn content and increases with wavelength.

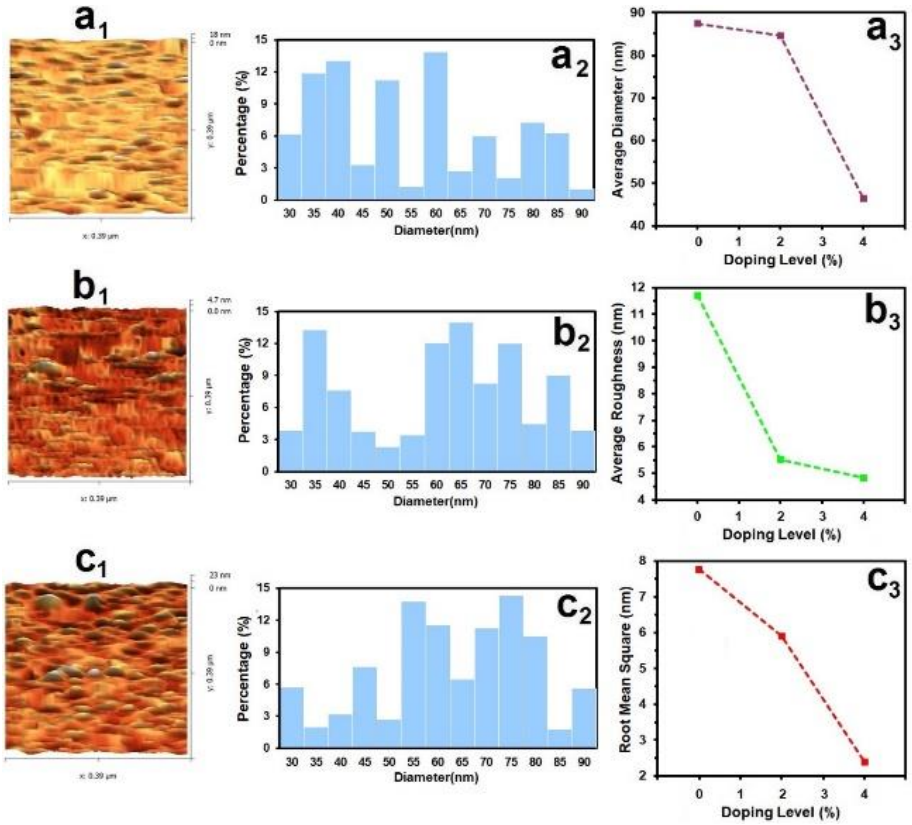

Figure 3: AFM surface morphology of undoped and Sn-doped NiO thin films.

The obtained values exceeding 10^4 cm^{-1} indicate strong optical absorption and confirm the presence of direct allowed electronic transitions in the films [45], [46]. The decrease in absorption coefficient with higher Sn doping suggests reduced light–matter interaction, likely due to modifications in the electronic structure and a lower density of states contributing to optical transitions.

The optical band gap was evaluated using the Tauc method [47], where the relationship between optical absorption and photon energy is analyzed. The corresponding plots are presented in Figure 7. The calculated band gap decreases from 3.86 eV to 3.75 eV with increasing Sn content [48], [49]. This reduction is attributed to the introduction of impurity levels within the band gap and increased carrier concentration, which leads to band tailing and narrowing of the optical gap. Such band gap tuning through doping is beneficial for optimizing the optical properties of NiO thin films for applications such as photovoltaics.

The extinction coefficient (k) describes the attenuation of an electromagnetic wave as it propagates through a material medium [50], [51]. The values of k were calculated using a standard optical relation involving the absorption coefficient and wavelength [52].

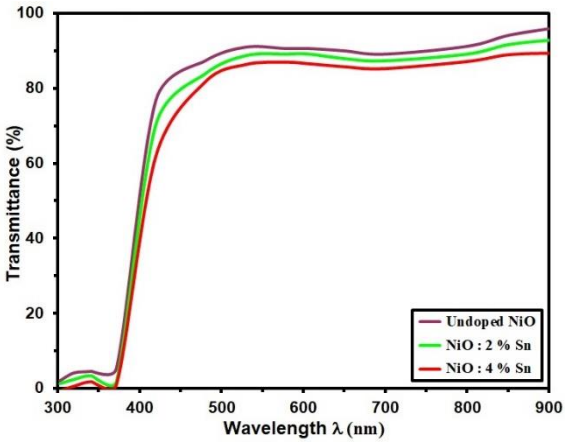

Figure 4: T of prepared films.

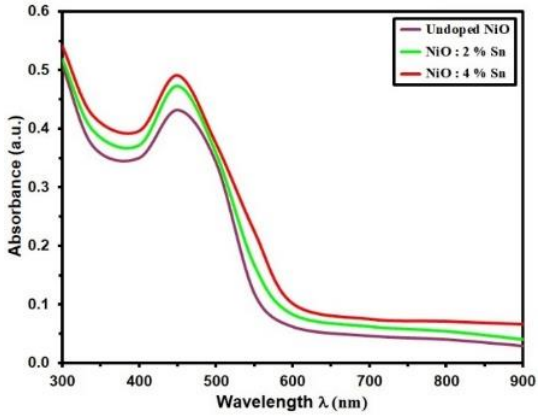

Figure 5: Absorbance of deposit films.

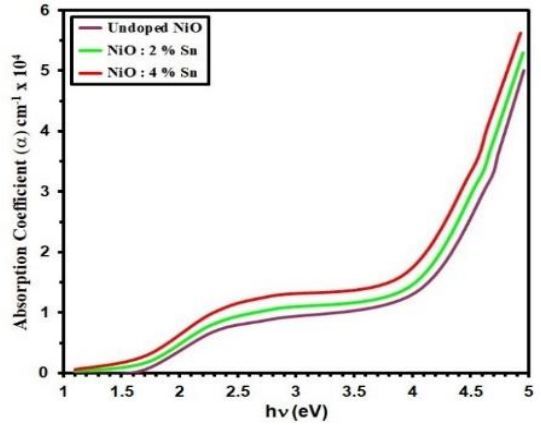

Figure 6: α Vs hν of intended films.

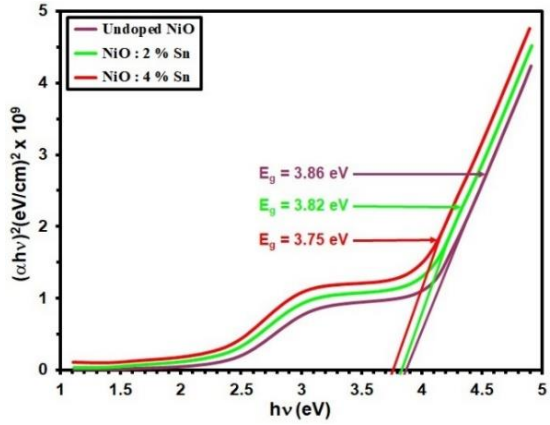

Figure 7: E_g of the prepared films.

Figure 8 illustrates the variation of the extinction coefficient for undoped and Sn-doped NiO films. It is observed that the extinction coefficient decreases with increasing tin concentration [53], [54]. This parameter provides information about how much light is absorbed per unit distance within the material. The reduction in k with higher Sn doping suggests decreased light absorption, which may be attributed to improved crystallinity, reduced defect density, or lower free carrier absorption. This trend indicates that tin doping enhances the optical transparency of NiO films, making them more suitable for optoelectronic applications such as transparent electrodes, solar cells, and optical coatings.

The complex refractive index was determined using a relation that incorporates both reflectance and extinction coefficient [55]. Figure 9 shows the spectral dependence of the refractive index for undoped and Sn-doped NiO films. The results indicate that the refractive index decreases with increasing Sn content [56]. This behavior is likely related to microstructural improvements such as enhanced crystallinity and reduced defect density. It may also be explained by a decrease in material polarizability due to the substitution of Ni^{2+} ions with Sn^{4+} ions [57].

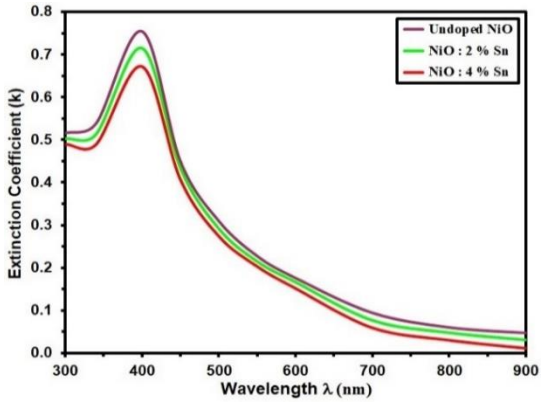

Figure 8: Extinction coefficient and Vs hν for intended films.

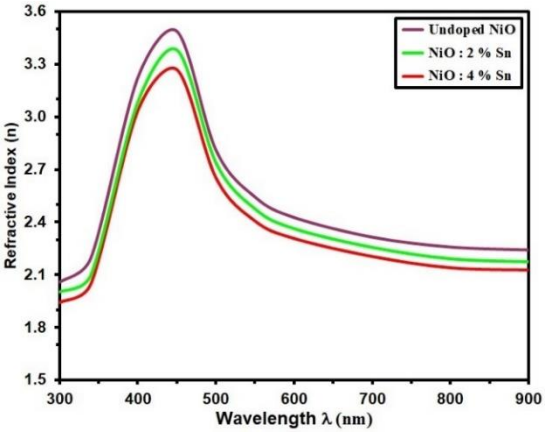

Figure 9: Refractive index Vs hν for intended films.

Figure 10 illustrates the change in resistance over response time. The observed reduction in resistance for all samples upon exposure to hydrogen gas (H_2) at a concentration of 225 ppm confirms that NiO behaves as a typical p-type semiconductor [18]. This behavior shows that hydrogen, acting as a reducing gas in this context, interacts with the film surface by donating electrons, which are captured by the material from the conduction band [58]. Additionally, the NiO film doped with 4% tin (Sn) exhibited the highest resistance, emphasizing the impact of doping concentration on the semiconductor properties of the films [13]. In p-type semiconductors, the primary charge carriers are holes. When exposed to a reducing gas like hydrogen, electron donation to the surface reduces recombination with holes, effectively increasing hole concentration. This leads to enhanced conductivity and thus lower resistance [58].

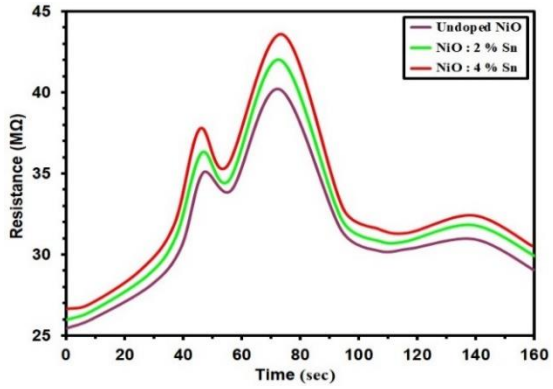

Figure 10: The resistance variation over time of the deposit films.

The sensor response, or detection sensitivity (S), is defined using a standard relation based on the change in resistance between gas-exposed and air conditions [59], [60].

The reduction in sensitivity with increasing tin content, as shown in the sensitivity curves in Figure 11 after exposure to hydrogen gas, can be explained by the increased electrical resistance of the films. This increase in resistance is associated with recombination processes involving charge carriers, including electrons and holes released from adsorbed oxygen species on the surface.

Specifically, the sensitivity decreases from 29.56% to 4.5% at 225 ppm, from 28.4% to 13.3% at 150 ppm, and from 27.3% to 12.3% at 75 ppm for undoped and Sn-doped NiO films, respectively. These results indicate that the doping concentration has a significant impact on the hydrogen gas sensing response, with higher Sn content leading to reduced sensitivity [60].

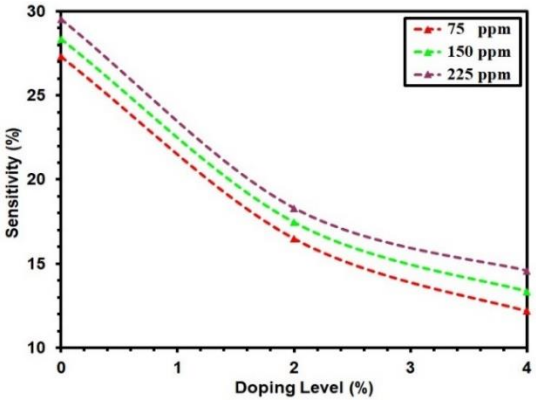

Figure 11: The sensitivity of the entended films.

4 CONCLUSIONS

The incorporation of tin (Sn) dopants significantly enhanced the crystalline quality of NiO thin films, as shown by increased grain size and decreased dislocation density and lattice strain. Surface characterization through AFM and SEM revealed that Sn doping promoted the formation of smoother, more uniform surfaces, with microstructural evolution from flat island formations to well-defined spherical nano-grains. Optical characterization showed a systematic reduction in bandgap energy from 3.86 eV to 3.75 eV, accompanied by a decrease in optical transmittance from 96.1% to 89.5%. These modifications were attributed to the introduction of defect states by Sn doping. Furthermore, the observed decrease in both extinction coefficient and refractive index indicated significant alterations in the optical interaction properties of the material. Regarding gas sensing performance, undoped NiO films displayed superior hydrogen sensitivity (29.56% at 225 ppm H_2), benefiting from their optimal surface-to-volume ratio. However, Sn-doped samples exhibited increased electrical resistance coupled with reduced sensitivity (4.5% for 4% Sn doping at 225 ppm), primarily due to enhanced charge carrier recombination processes.

ACKNOWLEDGMENTS

The authors are grateful to Mustansiriyah University (www.uomustansiriyah.edu.iq) for its assistance and for providing the requisite facilities for this research.

REFERENCES

[1] C. Parka, J. Kima, K. Leea, S. K. Oh, H. J. Kanga, and N. S. Park, "Electronic, Optical and Electrical Properties of Nickel Oxide Thin Films Grown by RF Magnetron Sputtering," Appl. Sci. Converg. Technol., vol. 24, pp. 72-76, 2015.

[2] H. Y. Ryu, G. P. Choi, W. S. Lee, and J. S. Park, "Preferred orientations of NiO thin films prepared by RF magnetron sputtering," J. Mater. Sci., vol. 39, no. 13, pp. 4375-4377, 2004.

[3] D. S. Kim and H. C. Lee, "Nickel vacancy behavior in the electrical conductance of nonstoichiometric nickel oxide film," J. Appl. Phys., vol. 112, pp. 1-5, 2012.

[4] H. Sato, T. Minami, S. Takata, and T. Yamada, "Transparent Conducting p-Type NiO Thin-Films Prepared by Magnetron Sputtering," Thin Solid Films, vol. 236, no. 1-2, pp. 27-31, 1993.

[5] S. D. Tiwari and K. P. Rajeev, "Magnetic properties of NiO nanoparticles," Thin Solid Films, vol. 505, pp. 113-117, 2006.

[6] K. C. Wang, P. S. Shen, M. H. Li, S. Chen, M. W. Lin, P. Chen, and T. F. Guo, "Low-temperature sputtered nickel oxide compact thin film as effective electron blocking layer for mesoscopic NiO/CH3NH3PbI3 perovskite heterojunction solar cells," ACS Appl. Mater. Interfaces, vol. 6, pp. 11851-11858, 2014.

[7] L. Ai, G. Fang, L. Yuan, N. Liu, M. Wang, C. Li, Q. Zhang, J. Li, and X. Zhao, "Influence of substrate temperature on electrical and optical properties of p-type semitransparent conductive nickel oxide thin films deposited by radio frequency sputtering," Appl. Surf. Sci., vol. 254, no. 8, pp. 2401-2405, 2008.

[8] M. Tadic, D. Nikolic, M. Panjan, and G. R. Blake, "Magnetic properties of NiO (nickel oxide) nanoparticles: Blocking temperature and Neel temperature," J. Alloys Compd., vol. 647, pp. 1061-1068, 2015.

[9] G. Cristina, L. D. Francis, M. M. Maurizio, C. Stefano, M. M. Francesco, P. Alfonso, I. Claudia, and S. Claudio, "Magneto-Plasmonic Colloidal Nanoparticles Obtained by Laser Ablation of Nickel and Silver Targets in Water," J. Phys. Chem. C, vol. 121, pp. 3597-3606, 2017.

[10] L. Zhao, G. Su, W. Liu, L. Cao, J. Wang, Z. Dong, and M. Song, "Optical and Electrochemical Properties of Cu-Doped NiO Films Prepared by Electrochemical Deposition," Appl. Surf. Sci., vol. 257, pp. 3974-3979, 2011.

[11] M. B. Islam, M. Yanagida, Y. Shirai, Y. Nabetani, and K. Miyano, "NiOx Hole Transport Layer for Perovskite Solar Cells with Improved Stability and Reproducibility," ACS Omega, vol. 2, no. 5, pp. 2291-2299, 2017.

[12] M. Arif, A. Sanger, M. Shkir, A. Singh, and R. S. Katiyar, "Influence of interparticle interaction on the structural, optical and magnetic properties of NiO nanoparticles," Phys. B, vol. 552, pp. 88-95, 2019.

[13] B. Pejova, T. Kocareva, M. Najdoski, and I. Grosdanov, "A solution growth route to nanocrystalline nickel oxide thin films," Appl. Surf. Sci., vol. 271, pp. 271-278, 2000.

[14] A. Agrawal, H. R. Habibi, R. K. Agrawal, J. P. Cronin, D. M. Roberts, R. Caron-Popowich, and C. M. Lampert, "Effect of deposition pressure on the microstructure and electrochromic properties of electron-beam-evaporated nickel oxide films," Thin Solid Films, vol. 221, no. 1-2, pp. 239-253, 1992.

[15] B .Sasi, K. G. Gopchandran, P. K. Manoj, P. Koshy, P. Prabhakara Rao, and V. K. Vaidyan, "Preparation of transparent and semiconducting NiO films," Vacuum, vol. 68, no. 2, pp. 149-154, 2002.

[16] S. Riad, S. A. Mahmoud, and A. A. Ibrahim, "Structural and DC electrical investigations of ZnO thin films prepared by spray pyrolysis technique," Physica B Condens. Matter, vol. 296, no. 4, pp. 319-325, 2001.

[17] Valyukh, S. Green, H. Arwin, G. A. Niklasson, E. Wäckelgård, and C. G. Granqvist, "Solar Energy Materials & Solar Cells," vol. 94, pp. 724-733, 2010.

[18] R. C. Korosec and P. Bukovec, "Sol-Gel Prepared NiO Thin Films for Electrochromic Applications," Acta Chim. Slov., vol. 53, no. 2, pp. 136-147, 2006.

[19] M. Tanaka, M. Mukai, Y. Fujimori, M. Kondoh, Y. Tasaka, H. Baba, and S. Usami, "Transition metal oxide films prepared by pulsed laser deposition for atomic beam detection," Thin Solid Films, vol. 281-282, pp. 453-456, 1996.

[20] L. Yang, Y. S. Lai, and J. S. Chen, "Effect of heat treatment on the properties of non-stoichiometric p-type nickel oxide films deposited by reactive sputtering," Thin Solid Films, vol. 488, p. 242, 2005.

[21] Fasaki, A. Koutoulaki, M. Kompitsas, and C. Charitidis, "Structural, electrical and mechanical properties of NiO thin films grown by pulsed laser deposition," Appl. Surf. Sci., vol. 257, p. 429, 2010.

[22] Y. M. Lu, W. S. Hwang, and J. S. Yang, "Properties of nickel oxide thin films deposited by RF reactive magnetron sputtering," Surf. Coat. Technol., vol. 155, p. 231, 2002.

[23] X. Wang and Z. Wei, "J. Adv. Microsc. Res.," vol. 10, p. 24, 2015.

[24] R. Sharma, A. D. Acharya, S. B. Shrivastava, M. Patidar, M. Gangrade, T. Shripathi, and V. Ganesan, "Studies on the structure optical and electrical properties of Zn-doped NiO thin films grown by spray pyrolysis," Optik, vol. 127, pp. 4661-4668, 2016.

[25] H. A. Juybari, M. M. Bagheri-Mohagheghi, and M. Shokooh-Saremi, "Nickel-lithium oxide alloy transparent conducting films deposited by spray pyrolysis technique," J. Alloys Compd., vol. 509, no. 6, pp. 2770-2775, 2011.

[26] Ravichandran and P. Philominathan, "Fabrication of antimony doped tin oxide (ATO) films by an inexpensive, simplified spray technique using perfume atomizer," Mater. Lett., vol. 62, pp. 2980-2983, 2008.

[27] W. Chia-Ching and Y. Cheng-Fu, "Nanoscale Res. Lett.," vol. 8, p. 33, 2013.

[28] N. N. Jandow, N. F. Habubi, S. S. Chiad, I. A. Al-Baidhany, and M. A. Qaeed, "Annealing Effects on Band Tail Width, Urbach Energy and Optical Parameters of Fe2O3:Ni Thin Films Prepared by Chemical Spray Pyrolysis Technique," Int. J. Nanoelectron. Mater., vol. 12, no. 1, pp. 1-10, 2019.

[29] M. A. Vidales-Hurtado and A. Mendoza-Galván, "Optical and Structural Characterization of Nickel Oxide-Based Thin Films Obtained by Chemical Bath Deposition," Mater. Chem. Phys., vol. 107, pp. 33-38, 2008.

[30] A. Bader, S. K. Muhammad, A. M. Jabbar, K. H. Abass, S. S. Chiad, and N. F. Habubi, "Synthesis and Characterization of Indium-doped CdO Nanostructured Thin Films: a Study on Optical, Morphological, and Structural Properties," J. Nanostruct., vol. 10, no. 4, pp. 744-750, 2020.

[31] A. Ibrahem, A. M. A. Karim, and T. H. Mubarak, "Study of the effect of cobalt on the structural properties of nickel ferrite prepared by chemical co-precipitation thermal method," Mater. Today Proc., 2023.

[32] W. A. Aelawi, S. Alptekin, and M. H. Al-Timimi, "Structural, optical, and electrical properties of nanocrystalline CdS1−xCuxS thin films," Indian J. Phys., vol. 97, no. 13, pp. 3949-3956, 2023.

[33] H. Sun, S. C. Chen, W. C. Peng, C. K. Wen, X. Wang, and T. H. Chuang, "The Influence of Oxygen Flow Ratio on the Optoelectronic Properties of p-Type NiO Films Deposited by Ion Beam Assisted Sputter," Coatings, vol. 8, p. 168, 2018.

[34] M. Kitao, K. Izawa, K. Urabe, T. Komatsu, S. Kuwano, and S. Yamada, "Preparation and electrochromic properties of rf-sputtered NiOx films prepared in Ar/O2/H2 atmosphere," Jpn. J. Appl. Phys., vol. 33, pp. 6656-6662, 1994.

[35] Tian, H. Deng, L. Sun, H. Kong, P. Yang, and J. Chu, "Effects of Co doping on structure and optical properties of TiO2 thin films prepared by sol-gel method," Thin Solid Films, vol. 520, no. 16, pp. 5179-5183, 2012.

[36] Tauc, R. Grigorovici, and A. Vancu, "Optical properties and electronic structure of amorphous germanium," Phys. Status Solidi B, vol. 15, no. 2, pp. 627-637, 1966.

[37] J. D. Desai, S. K. Min, K. D. Jung, and O. S. Joo, "Spray pyrolytic synthesis of large area NiOx thin films from aqueous nickel acetate solutions," Appl. Surf. Sci., vol. 253, no. 4, pp. 1781-1786, 2006.

[38] Cattin, B. A. Reguig, A. Khelil, M. Morsli, K. Benchouk, and J. C. Bernede, "Properties of NiO thin films deposited by chemical spray pyrolysis using different precursor solutions," Appl. Surf. Sci., vol. 254, pp. 5814-5821, 2008.

[39] X. H. Xia, J. P. Tu, J. Zhang, X. L. Wang, W. K. Zhang, and H. Huang, "Electrochromic properties of porous NiO thin films prepared by a chemical bath deposition," Sol. Energy Mater. Sol. Cells, vol. 92, pp. 628-633, 2008.

[40] T. H. Mubarak, K. H. Hassan, and Z. M. A. Abbas, "Using X-ray diffraction and scanning electron microscope to study zinc oxide nanoparticles prepared by wet chemical method," Adv. Mater. Res., vol. 685, pp. 119-122, 2013.

[41] T. Manago, T. Ono, H. Miyajima, I. Yamaguchi, K. Kawaguchi, and M. Sohma, "Thin Solid Films," vol. 374, pp. 21-26, 2004.

[42] F. Habubi, K. H. Abass, S. Chiad, D. M. A. Latif, J. N. Nidhal, and A. I. Al-Baidhany, "Dispersion Parameters of Polyvinyl Alcohol Films doped with Fe," J. Phys. Conf. Ser., vol. 1003, no. 1, p. 012094, 2018.

[43] H. Kumagai, M. Matsumoto, K. Toyoda, and M. Obara, "Preparation and characteristics of nickel oxide thin film by controlled growth with sequential surface chemical reactions," J. Mater. Sci. Lett., vol. 15, pp. 1081-1083, 1996.

[44] Ristova, J. Velveska, and M. Ristov, "Chemical bath deposition and electrochromic properties of NiOx films," Sol. Energy Mater. Sol. Cells, vol. 71, pp. 219-230, 2002.

[45] Y. M. Lu, W. S. Hwang, and J. S. Yang, "Effects of substrate temperature on the resistivity of non-stoichiometric sputtered NiOx films," Surf. Coat. Technol., vol. 155, pp. 231-235, 2002.

[46] S. S. Chiad, A. S. Alkelaby, and K. S. Sharba, "Optical Conduct of Nanostructure Co3O4 rich highly doping Co3O4:Zn alloys," J. Glob. Pharma Technol., vol. 11, no. 7, pp. 662-665, 2020.

[47] Jlassi, I. Sta, M. Hajji, and H. Ezzaouia, "Synthesis and characterization of nickel oxide thin films deposited on glass substrates using spray pyrolysis," Appl. Surf. Sci., vol. 308, pp. 199-205, 2014.

[48] A. Boukhachem, R. Boughalmi, M. Karyaoui, A. Mhamdi, R. Chtourou, K. Boubaker, and M. Amlouk, "Study of substrate temperature effects on structural, optical, mechanical and opto-thermal properties of NiO sprayed semiconductor thin films," Mater. Sci. Eng. B, vol. 188, pp. 72-77, 2014.

[49] H. Kamel, E. K. Elmaghraby, S. A. Ali, and K. Abdel-Hady, "The Electrochromic Behavior of Nickel Oxide Films Sprayed at Different Preparative Conditions," Thin Solid Films, vol. 483, no. 1-2, pp. 330-339, 2005.

[50] A. Al-Ghamdi, W. E. Mahmoud, S. J. Yaghmour, and F. M. Al-Marzouki, "Structure and Optical Properties of Nanocrystalline NiO Thin Film Synthesized by Sol-Gel Spin-Coating Method," J. Alloys Compd., vol. 486, no. 1-2, pp. 9-13, 2009.

[51] S. S. Chiad, H. A. Noor, O. M. Abdulmunem, and N. F. Habubi, "Optical and structural properties of Ni-doped Co3O4 nanostructure thin films via CSPM," J. Phys. Conf. Ser., vol. 1362, no. 1, 2019.

[52] Abdullah and Khairurrijal, "Derivation of Scherrer relation using an approach in basic physics course," J. Nanosci. Nanotechnol., vol. 1, no. 1, pp. 28-32, 2008.

[53] W. A. Zoba, "Structural, Optical and Electrical Properties for NiO Thin Films Prepared by Pulsed Laser Deposition," Int. J. ChemTech Res., vol. 9, no. 12, pp. 791-798, 2016.

[54] S. S. Chiad, H. A. Noor, O. M. Abdulmunem, N. F. Habubi, M. Jadan, and J. S. Addasi, "Optical and structural performance of nanostructured Te thin films by CSP with various thicknesses," J. Ovonic Res., vol. 16, no. 1, pp. 35-40, 2020.

[55] S. D. Tiwari and K. P. Rajeev, "Magnetic properties of NiO nanoparticles," Thin Solid Films, vol. 505, pp. 113-117, 2006.

[56] Arif, A. Sanger, M. Shkir, A. Singh, and R. S. Katiyar, "Influence of interparticle interaction on the structural, optical and magnetic properties of NiO nanoparticles," Phys. B, vol. 552, pp. 88-95, 2019.

[57] Adler and J. Feinleib, "Electrical and optical properties of narrow-band materials," Phys. Rev. B, vol. 2, p. 3112, 1970.

[58] S. R. Nalage, M. A. Chougule, S. Sen, P. B. Joshi, and V. B. Patil, “Sol-gel synthesis of nickel oxide thin films and their characterization,” Thin Solid Films, vol. 520, pp. 4835-4840, 2012.

[59] Vera, R. Schrebler, E. Munoz, C. Suarez, P. Cury, A. Gomez, R. Cordova, R. E. Marotti, and E. A. Dalchiele, “Preparation and characterization of Eosin B- and Erythrosin J-sensitized nanostructured NiO thin film photocathodes,” Thin Solid Films, vol. 490, pp. 182-188, 2005.

[60] L. Barkat, L. Cattin, A. Reguig, M. Regragui, and J. C. Bernede, “Comparison of the physico-chemical properties of NiO thin films deposited by chemical bath deposition and by spray pyrolysis,” Mater. Chem. Phys., vol. 89, pp. 11-20, 2005.